Contents lists available at ScienceDirect

Spectrochimica Acta Part A: Molecular and Biomolecular Spectroscopy

journal homepage: www.elsevier.com/locate/saa

Crystal structure, thermal and spectral studies and growth of nonlinear optical *L*-lysinium fluoride crystal
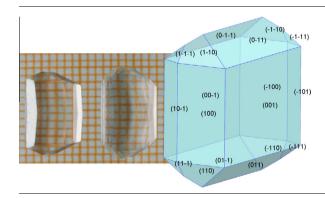
R.P. Sukiasyan [a,*], H.A. Karapetyan [b], A.K. Atanesyan [a], R.A. Apreyan [a]

[a] Laboratory of the Crystal Growth, Institute of Applied Problems of Physics, NAS of Armenia, Hr. Nersessyan St 25, Yerevan 0014, Armenia
[b] Molecule Structure Research Center, NAS of Armenia, Azatutyan Ave., 26, Yerevan 0014, Armenia

HIGHLIGHTS

- The structural, spectroscopic, optical and thermal properties of *L*-Lys·HF were studied.
- High quality *L*-Lys·HF single crystals were grown from aqueous solution.
- *L*-Lys·HF crystals are enough thermostable.

GRAPHICAL ABSTRACT

ABSTRACT

In current study properties of *L*-lysinium fluoride (*L*-Lys·HF) are determined by X-ray diffraction, infrared and Raman spectroscopy, SHG and by UV–vis transmittance spectrum measurement. *L*-Lys·HF ($C_6H_{15}FN_2O_2$), crystallizes in a monoclinic system with space group P2$_1$, $a = 5.464(1)$ Å, $b = 7.4717(15)$ Å, $c = 10.252(2)$ Å, $\alpha = \gamma = 90°$, $\beta = 99.17(3)°$, $Z = 2$, $\rho_c = 1.336$ Mg/m^3, $\rho_m = 1.335(2)$ Mg/m^3. By means of evaporation method high quality *L*-Lys·HF single crystals are grown from aqueous solutions. *L*-Lys·HF rystal is transparent in the wavelength region 240–1100 nm and it exhibits powder SHG efficiency 0.65 times that of potassium dihydrogen phosphate (KDP).

© 2013 Elsevier B.V. All rights reserved.

Introduction

Crystalline salts of optically active amino acids (e.g. *L*-arginine [1,2], *L*-lysine [3–13], etc.) have been intensively studied as nonlinear optical (NLO) materials for last years. *L*-arginine fluoride reveals nonlinear optical properties almost not conceding to that of *L*-arginine phosphate (LAP): second harmonic generation efficiencies $I/I_0 = 6.0$ and 5.6 for LAP and *L*-arginine fluoride, respectively [1].

L-lysine (*L*-Lys) has functional groups similar to *L*-arginine. Suzuki and Matsuoka [3] reported that NLO activity of *L*-lysine salts is two–three times higher than that of KDP. They obtained crystals of phosphate, iodate and borate salts of *L*-lysine. Marchewka et al. [8] prepared some new NLO active *L*-lysine salts of *L*-tartaric, acetic, arsenous, fumaric acids. Growth and characterization of the nonlinear optical single crystals of *L*-lysine acetate and *L*-Lysine trifluoroacetate were reported by Sun et al. [9,10].

Until now more than fifty salts of lysine are known, 90% of which are of organic acids with complicated structures, mainly synthesized as food additives.

* Corresponding author. Tel.: +374 10 240423; fax: +374 10 281861.
E-mail address: ruzas@iapp.sci.am (R.P. Sukiasyan).

Further research of new *L*-lysine salts as NLO materials is reported by Sukiasyan [11], where the interactions of *L*-lysine with HF, HNO₃, HBF₄, HClO₄, HCOOH and H₂C₂O₄ [12] acids are studied. Sukiasyan showed that in the *L*-Lys + HF + aq system, three compounds are formed as identified by IR spectra. The most interesting of these compounds is *L*-Lys·HF, which is obtained as a single crystal.

In this paper, we report results of structure determination for *L*-Lys·HF by X-ray diffraction. Thermal, nonlinear optical properties and infrared, Raman, UV–vis transmittance spectra of *L*-Lys·HF are shown and discussed.

Experimental part

Selected starting reagents, *L*-lysine (*L*-Lys) (H₂N(CH₂)₄CH(NH₂)COOH), were synthesized and purified in the Institute of Biotechnology (Yerevan); commercially obtained fluoric acid (HF, 40% solution, "chem. pure" grade) was used.

For determination of thermal properties Paulik–Paulik–Erdey Derivatograph (MOM, Hungary, temperature range: 20–500 °C, specimen mass: 81.3 mg, heating rate: 5 °C/min in air atmosphere) as well as Boëtius type microscope with heated stage (in the range 20–350 °C) were used.

X-ray diffraction data for structure analysis were collected by a CAD-4 Enraf Nonius diffractometer. We used the SHELXS 97 and SHELXL 97 programs [14,15] for structure resolution and refinement.

Fourier-transform Raman spectra were registered by a NXP FT-Raman Module of a Nicolet 5700 spectrometer (number of scans 256, resolution 4 cm⁻¹). The same spectrometer was used for measuring IR spectra with nujol (4000–400 cm⁻¹, number of scans 32, resolution 2 cm⁻¹). Attenuated total reflection of Fourier-transform infrared spectra (FTIR ATR) were registered by a Nicolet "Nexus" FT-IR spectrometer with ZnSe prism (4000–650 cm⁻¹, number of scans 16, resolution 4 cm⁻¹). The UV–vis transmittance was measured by a "Helios Gamma" UV–vis spectrophotometer (England).

For checking the nonlinear optical activity by the powder Kurtz–Perry method, a YAG:Nd laser (passive Q-switching, duration of pulses 20 ns, repetition rate 8 Hz) was used (for details see [19]).

Results and discussion

Synthesis and crystal growth

Colourless crystals of *L*-Lys·HF are obtained by slow evaporation of the aqueous solution of *L*-Lys:HF ratio in 2:1–1:1.5 interval within 0–40 °C temperature range. The sample can be recrystallized in the mentioned temperature interval.

High quality *L*-Lys·HF single crystals with dimensions 10 × 7 × 3.5 and 12 × 8 × 4 mm³ (see Fig. 1) were grown in a plastic vessel by slow evaporation of the solvent from aqueous solution at the temperature of 34 °C (growth rate is 0.9 × 0.5 × 0.2 mm³/day and 0.8 × 0.5 × 0.2 mm³/day respectively). The morphology of the grown single crystals very well coincides with the one painted by the Mercury 2.4 program (see Fig. 1). At the temperature of 20 °C pH of the saturated solution of *L*-Lys·HF equals 4.

Crystal and molecular structure of *L*-Lys·HF

The compound *L*-Lys·HF crystallizes in monoclinic system with space group P2₁. Crystallographic data and details of refinement of the structure are given in Table 1. Asymmetric part of a unit cell and atomic numbering scheme is shown in Fig. 2. Characteristic
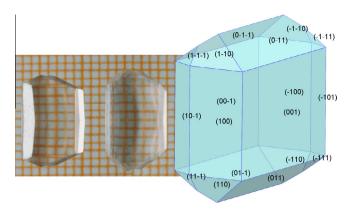

Fig. 1. The single crystals and crystal morphology of *L*-lysinium fluoride.

interaction pattern in *L*-Lys·HF forming a layer parallel to the bc plane is shown in Fig. 3. Intramolecular bond lengths and angles are given in Table 2. All H atoms were positioned geometrically and refined using riding model with C–H = 0.97/%A and Uiso(H) = 1.2 eq(C), N–H = 0.89/%A and Uiso(H) = 1.5 eq(N). Hydrogen bond parameters are given in Table 3. Torsion angles of lysinium cation are given in Table 4.

Values of bond lengths C(1)–O(1) and C(1)–O(2) equal to 1.238(3) Å and 1.247(2) Å, accordingly, which indicates the negatively charged C(1)OO⁻ carboxylate group. Values of bond lengths and angles are in accordance with standard values and therefore we can conclude that *L*-lysine moiety is in state of singly charged *L*-Lys⁺ cation. Amino groups of lysinium cation are protonated due to hydrogens of the COOH group and HF. Thus, the formation mechanism of *L*-Lys·HF can be described as *L*-Lys⁺·F⁻.

Lysinium cations aggregate into layers. In each layer (see Fig. 3), the most prominent feature is the linear arrays of lysinium cations stabilized by strong hydrogen bonds between amino groups and F⁻ anions. Lysinium cations are arranged in linear arrays along c axis. Molecules in the array are related by a translation. Adjacent arrays, related by a 2₁ screw axis, run in opposite directions. They are interconnected by hydrogen bonds involving the side-chain amino group and carboxylate O atoms. All hydrogen atoms of the α- and ε-amino NH₃⁺ groups of the *L*-Lys⁺ cation form hydrogen bonds. There are three hydrogen bonds between two amino groups and the COO⁻ group of lysinium cations. The H(2A) and H(2B) atoms of N(2) atom are connected to O(1) and O(2) atoms of lysinium cations of adjacent arrays by means of rather strong N(2)–H(2A)···O(1) and weak N(2)–H(2B)···O(2) hydrogen bonds (see Table 3, Fig. 3), according to Zefirov [16]. There is a third rather strong N(1)–H(1A)···O(2) hydrogen bond, with the H(1A)···O(2) distance equals 1.96 Å, between lysinium cations of adjacent layers parallel to the bc plane.

F⁻ anions are located between lysinium cations related by a translation approximately at equal distances (see Fig. 3). A F⁻ anion is connected to a N(2) atom of lysinium cation and to N(1) atoms of symmetrically equivalent lysinium cations by means of strong N(2)–H(2C)···F, N(1)–H(1B)···F and N(1)–H(1C)···F hydrogen bonds with N···F distances equal to 2.628(2) Å, 2.630(2) Å and 2.722(2) Å, respectively (see Table 3).

Such interactions lead to one or more head-to-tail sequences similar to some lysine salts, for example [17].
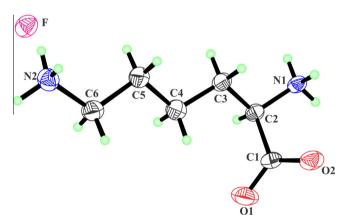
Thermal properties

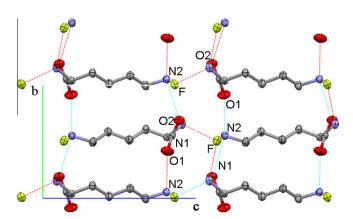Thermogravimetric (TG), derivative thermogravimetric (DTG) and differential thermoanalytical (DTA) curves are shown in

Table 1
Crystal data and structure refinement for *L*-Lys·HF.

Empirical formula	$C_6H_{15}FN_2O_2$
Formula weight	166.20
Temperature (K)	293(2)
Wavelength (Å)	0.71073
Crystal system	Monoclinic
Space group	$P2_1$
Unit cell dimensions	$a = 5.464(1)$ Å, $b = 7.4717(15)$ Å, $c = 10.252(2)$ Å, $\alpha = 90°$, $\beta = 99.17(3)°$, $\gamma = 90°$
Volume (Z)	413.2(1) Å^3, 2
Density (calculated)	$D_c = 1.336$ Mg/m^3
Density (measured)	$D_m = 1.335(2)$ Mg/m^3
Absorption coefficient	0.113 mm^{-1}
$F(000)$	180
Crystal size	$0.21 \times 0.14 \times 0.11$ mm^3
θ Range for data collection	$2.01 \div 28.96°$
Index ranges	$0 \leqslant h \leqslant 7, 0 \leqslant k \leqslant 10, -13 \leqslant l \leqslant 13$
Reflections collected	1278
Independent reflections	1168 ($R_{int} = 0.0183$)
Refinement method	Full-matrix least-squares on F^2
Data/restraints/parameters	1168/1/103
Goodness-of-fit on F^2	1.050
Final R indices [$I > 2\sigma(I)$]	$R1 = 0.0314$, $wR2 = 0.0820$
R indices (all data)	$R1 = 0.0415$, $wR2 = 0.0859$
Largest diff. peak and hole	0.205 and -0.137 eÅ^{-3}

CCDC 890479 contains the supplementary crystallographic data for this paper. These data can be obtained free of charge via www.ccdc.cam.ac.uk/conts/retrieving.html (or from the cambridge crystallographic data centre, 12 union road, cambridge CB2 1EZ, UK; fax: +44 1223 336033).

Fig. 2. The asymmetric unit of *L*-Lys·HF and atomic numbering scheme.

Fig. 3. Lysinium cations aggregate into layers in *L*-Lys·HF parallel to the bc plane. Only atoms involved in the hydrogen-bonding scheme are labelled.

Table 2
Bond lengths (Å) and angles (°) for *L*-Lys·HF.

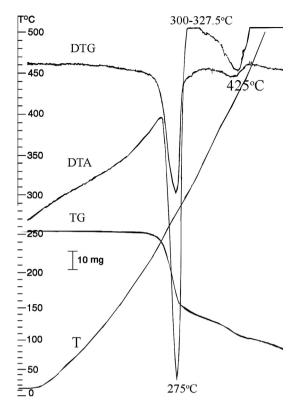|			
O(1)–C(1)	1.238(3)	O(1)–C(1)–O(2)	124.9(2)
O(2)–C(1)	1.247(2)	O(1)–C(1)–C(2)	118.0(2)
N(1)–C(2)	1.486(2)	O(2)–C(1)–C(2)	117.1(2)
N(2)–C(6)	1.481(2)	N(1)–C(2)–C(1)	108.6(1)
C(1)–C(2)	1.535(2)	N(1)–C(2)–C(3)	108.45(15)
C(2)–C(3)	1.530(2)	N(2)–C(6)–C(5)	113.2(2)
C(3)–C(4)	1.525(2)	C(1)–C(2)–C(3)	112.0(1)
C(4)–C(5)	1.524(3)	C(2)–C(3)–C(4)	113.0(2)
C(5)–C(6)	1.508(3)	C(3)–C(4)–C(5)	113.4(2)
		C(4)–C(5)–C(6)	109.69(15)

Table 3
Hydrogen bonds parameters in the structure of *L*-Lys·HF.

D–H···A	Symmetry code of A	D···A (Å)	H···A (Å)	D–H (Å)	D–H–A (°)
N(1)–H(1A)···O(2)	$x-1, y, z$	2.823(2)	1.96	0.89	163.9
N(1)–H(1B)···F	$x, y, z-1$	2.630(2)	1.75	0.89	169.3
N(1)–H(1C)···F	$-x+1, y+1/2, -z+1$	2.722(2)	1.85	0.89	167.1
N(2)–H(2A)···O(1)	$-x+2, y+1/2, -z+1$	2.745(3)	1.87	0.89	165.2
N(2)–H(2B)···O(2)	$-x+2, y-1/2, -z+1$	2.917(2)	2.22	0.89	134.6
N(2)–H(2C)···F	x, y, z	2.628(2)	1.74	0.89	176.2
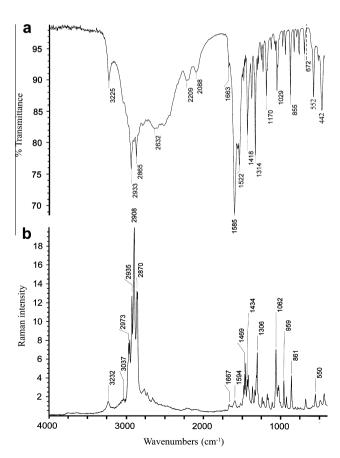
Table 4
Torsion angles of lysinium cation of *L*-Lys·HF.

N(1)–C(2)–C(1)–O(1) [Ψ^1]	−151.5(2)
N(1)–C(2)–C(3)–C(4) [χ^1]	−173.65(15)
C(2)–C(3)–C(4)–C(5) [χ^2]	179.6(2)
C(3)–C(4)–C(5)–C(6) [χ^3]	−176.0(2)
C(4)–C(5)–C(6)–N(2) [χ^4]	−177.8(2)

Fig. 4. We also observed the processes occurring in the 20–350 °C interval by a microscope with heating stage.

In the temperature interval of 149–200 °C (DTG peak at 162 °C), mass loss determined by TG curve is equal to 1%, which in our opinion is related to adsorbed H_2O or HF. However, the observation of heating process of transparent single crystalline *L*-Lys·HF sample indicated that at the heating point of up to 200 °C the sample does not show any changes. The latter is also confirmed by the IR spectrum of heated sample that does not show any changes as well.

Fig. 4. Thermogravimetric (TG), derivative thermogravimetric (DTG) and differential thermoanalytical (DTA) curves of L-Lys·HF (the mass of specimen 81.3 mg).

Fig. 5. FTIR ATR (a) and FT Raman (b) spectra of L-Lys·HF (spectrum in the region 650 ÷ 400 cm^{-1} was registered with nujol).

According to DTA curve, first decomposition of L-Lys·HF occurs with endothermic process in the 210–282 °C interval (DTA peak at 275 °C). Mass loss determined by TG curve is equal to 49.2%. So, L-Lys·HF crystals are reasonably thermostable. With further heating, the decomposition occurs in the 300–328 °C interval with an exothermic process. Further complete decomposition occurs with DTA peak at 425 °C.

Vibration spectra

Vibration spectra of L-Lys·HF are shown in Fig. 5. Values of wavenumbers are collected in Table 5 together with the assignment of some characteristic bands.

On the basis of correlation between the vibrational frequencies of N–H bonds and N$\cdots$O, N$\cdots$F distances [18], it is estimated the expected values of wavenumbers of ν(NH) vibrations. The absorption bands in the IR spectrum of L-Lys·HF (Fig. 4) at 3225 cm^{-1} and 3037 cm^{-1} as well as respective Raman-lines at 3232 cm^{-1} and 3037 cm^{-1} are assigned to stretching vibrations ν(NH) of NH$_3^+$ groups for weak N(2)–H(2B)$\cdots$O(2) and N(1)–H(1A)$\cdots$O(2) hydrogen bonds (see Tables 3 and 5). For rather strong N(1)–H(1B)$\cdots$F, N(2)–H(2C)$\cdots$F and N(1)–H(1C)$\cdots$F hydrogen bonds, it is expected the ν(NH) wavenumbers around 2600 cm^{-1} and 2780 cm^{-1}, respectively. In the IR spectrum broad band with peaks at 2632 cm^{-1}, 2597 cm^{-1} and 2782 cm^{-1} as well as respective Raman-lines at 2768 cm^{-1} and 2657 cm^{-1} corresponds to the position of bands caused by stretching vibrations of strong N–H$\cdots$F hydrogen bonds. The very strong bands with peaks at 2973 cm^{-1}, 2960 cm^{-1}, 2935 cm^{-1}, 2908 cm^{-1}, 2870 cm^{-1} and 2862 cm^{-1} in the Raman spectrum are assigned to stretching ν(C–H) vibrations of CH and CH$_2$ groups. In the 2800–1800 cm^{-1} region, where the

Table 5
Wavenumbers (cm^{-1}) of vibrational spectra of L-Lys·HF.

ATR IR	Raman	Assignment
3225	3232	ν(N(2)–H(a))
3037 sh	3037	ν(NH) NH$_3^+$
2933; 2898	2973; 2960; 2935; 2908	ν_{as}(CH)CH$_2$
2865	2870; 2862	ν_s(CH)CH$_2$
2840 sh		ν(CH) CH
2782	2768	ν(N(1)–H(b))
2725	2728	Overtones and combinational bands
2632	2657	ν(N(1)–H(a))
2597	2603	ν(N(2)–H(b))
2548; 2511; 2209; 2088	2224; 2102	Overtones and combinational bands
1663	1667	ν_{as}(COO$^-$)
1651sh; 1632sh; 1585; 1558; 1548; 1539	1641; 1594; 1548	δ_{as}(NH$_3^+$)
1522	1518	δ_s(NH$_3^+$)
1482; 1465; 1452; 1439	1480; 1469; 1456; 1434	δ(CH$_2$)
1418	1422	ν_s(COO$^-$)
1361; 1328sh; 1314	1366; 1335; 1317; 1306	ω(CH$_2$)
1286; 1273; 1236; 1213	1239; 1222	τ(CH$_2$)
1170; 1157	1174; 1160	ρ(NH$_3^+$)
1105; 1064; 1049; 1031; 1020	1108; 1062; 1035; 1025	ν(C–N)
1001sh; 955; 921	1003; 959; 925	ν(C–C)
889; 855; 806	861; 809	ν(C–C) + γ(C–H)
773	778	δ(COO$^-$)
744; 739	742	ρ(CH$_2$)
672	676	ω(COO$^-$)
580sh; 552; 521	583; 550	ρ(COO$^-$)
490; 477sh; 440; 404	489; 435; 345; 257; 227	

ν – Stretching, δ – deformation scissoring, ω – wagging, τ – twisting, ρ – rocking, γ – out-of-plane bending, s – symmetric, as – asymmetric, sh – shoulder.
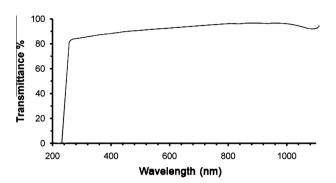
Fig. 6. Transmittance spectrum of *L*-lysinium fluoride.

weak bands caused by overtones and combinational tones are usually observed, in addition to broad band with peaks at 2632 cm^{-1}, 2597 cm^{-1} and 2782 cm^{-1}, bands near 2209 cm^{-1}, 2088 cm^{-1} (Fig. 4) are found as well. Absorption bands in the 1600–1500 cm^{-1} region are caused by the asymmetric stretching vibration of carboxylate group and asymmetric deformation vibration of NH$_3^+$ groups. The absorption band of COO$^-$ is shifted to the higher frequency side because of the presence of NH$_3^+$ group. Thus, the absorption band in the IR spectrum at 1663 cm^{-1} as well as respective Raman-line at 1667 cm^{-1} are assigned to asymmetric stretching vibration of carboxylate group.

So, the absence of the absorption band near 1700 cm^{-1} of COOH group and the existence of the absorption band of NH$_3^+$ group in the vibrational spectra of this crystal show that the lysine moiety is in form of a singly charged cation Lys$^+$ and hydrofluoric acid is in form of a F$^-$ ion.

Optical properties

From a crystal of optical quality a plate with a thickness of 0.8 mm was cut. In Fig. 6, transmittance spectrum in the range 200–1100 nm is shown. Absorption edge is located near 232 nm. Any absorption bands are absent in the 240–1100 nm range.

SHG efficiency of *L*-Lys·HF crystal powder was estimated as $I = 0.65\ I_{KDP}$ ($I = 3.5$, $I_{KDP} = 6.75$).

Conclusions

The compound *L*-Lys·HF crystallizes in monoclinic system with space group P2$_1$.

The structure of *L*-Lys·HF can be described as *L*-Lys$^+$·F$^-$. This crystal is characterised by IR and Raman spectra. *L*-Lys·HF crystal is reasonably thermostable. High quality *L*-Lys·HF single crystals were grown by evaporation method. Optical studies confirmed that *L*-Lys·HF crystal is transparent in the wavelength region 240–1100 nm. Second harmonic generation efficiency is $I/I_{KDP} = 0.65$ for *L*-Lys·HF.

Acknowledgements

References

[1] S.B. Monaco, L.E. Davis, S.P. Velsko, F.T. Wang, D. Eimerl, A. Zalkin, J. Cryst. Growth 85 (1987) 252–255.
[2] A.M. Petrosyan, R.P. Sukiasyan, H.A. Karapetyan, S.S. Terzyan, R.S. Feigelson, J. Cryst. Growth 213 (2000) 103–111.
[3] A. Suzuki, Y. Matsuoka, Jpn. Kokai Tokkyo koho JP 03 03, 834 [9133,834] (Cl. G02 F1/35) 14.02.1991, appl. 89/168, 872; 4 pp.
[4] A.M. Petrosyan, R.P. Sukiasyan, S.S. Terzyan, V.M. Burbelo, Acta Crystallogr. B55 (1999) 221–225.
[5] A.M. Petrosyan, S.S. Terzyan, V.M. Burbelo, R.P. Sukiasyan, Z. Naturforschung 53a (1998) 528–536.
[6] A.G. Nalbandyan, R.P. Sukiasyan, E.V. Novikov, E.W. Van Stryland, A.M. Petrosyan, Proc. Conf. on "Laser Physics-99", October 18–22, 1999, Ashtarak, Armenia, 2000, pp. 128–132.
[7] A.M. Petrosyan, V.M. Burbelo, R.A. Tamazyan, H.A. Karapetyan, R.P. Sukiasyan, Z. Naturforschung 55a (2000) 199–206.
[8] M.K. Marchewka, S. Debrus, H. Ratajczak, Cryst. Growth Des. 3 (2004) 587–592.
[9] Z.H. Sun, G.H. Zhang, X.Q. Wang, X.F. Cheng, X.J. Liu, L.Y. Zhu, H.L. Fan, G. Yu, D. Xu, J. Cryst. Growth 310 (2008) 2842–2847.
[10] Z.H. Sun, D. Xu, X.Q. Wang, G.H. Zhang, G. Yu, L.Y. Zhu, H.L. Fan, Mater. Res. Bull. 44 (2009) 925–930.
[11] R.P. Sukiasyan, Proc. Conf. on "Laser Physics-2004", October 12–15, 2004, Ashtarak, Armenia, 2005, pp. 105–108.
[12] R.P. Sukiasyan, H.A. Karapetyan, A.M. Petrosyan, J. Mol. Struct. 888 (2008) 230–237.
[13] A.M. Petrosyan, V.V. Ghazaryan, J. Mol. Struct. 917 (2009) 56–62.
[14] G.M. Sheldrick, SHELXL97. Program for the refinement of crystal structures, University of Göttingen, Germany, 1997.
[15] G.M. Sheldrick, SHELXS97. Program for the solution of crystal structures, University of Göttingen, Germany, 1997.
[16] Yu.V. Zefirov, Kristallografia 44 (1999) 1091–1093.
[17] A. Sharma, S. Thamotharan, S. Roy, M. Vijayan, Acta Crystallogr. C62 (2006) o148–o152.
[18] Novak, in: Infrared and Raman Spectroscopy of Biological Molecules. Proc. NATO Advanced Study Institute, Athens, Greece, August 22–31, 1978. Dordrecht, 1979, pp. 279–303.
[19] H.A. Petrosyan, R.A. Apreyan, A.A. Hovhannesyan, A.K. Atanesyan, A.M. Petrosyan, J. Contemp. Phys. (Armenian Acad. Sci.) 44 (2009) 43–49.